

GBT Pulsar Spigot Card Test Results: 2003-August

D. Kaplan, R. Escoffier, R. Lacasse, F. Ghigo, S. Ransom, I. Stairs, B. Jacoby

We tested the GBT Pulsar Spigot Card system a number of ways:

1. Checked operation of 4, 8, and 16-bit modes with a narrow input pulse synched to the spectrometer clocks. This verified that we were packing the lags in the correct order.
2. Checked operation of 4, 8, and 16-bit modes with a broad noise source, after determining scale and offset factors. This verified that we could correctly determine the statistics of the incoming data.
3. Checked operation of 4, 8, and 16-bit modes with several pulsars. The pulse-profiles and signal-to-noise ratios of the different modes were the same.
4. Observed PSR B1929+10 simultaneously with the Spigot and BCPM. The barycentric periods measured by each machine were identical to the precision of the measurements ($0.25 \mu\text{s}$).
5. Observed several pulsars at different frequencies, demonstrating the higher available bandwidths at $\nu_{\text{RF}} > 1.4 \text{ GHz}$.
6. Observed several millisecond binary pulsars repeatedly at different orbital phases, verifying that the TOAs were consistent with the established timing models.

The pulsar observations are summarized in Table 1, and we present pulse profiles in Figures 1–5. All processing was done with PRESTO using the best available ephemerides. In several cases we also show the profiles from the EPN¹ database, and the profiles from the Spigot agree with those from the archive.

Lags can be transmitted from the correlator with either 2, 4, 8, or 16-bit precision, depending on the mode. Before the data are truncated, though, they are offset and scaled according to values in a memory bank (the values can differ for each lag). Some of the observations were taken without setting the lag scales and offsets (just accepting the default values), which gives non-optimal dynamic range and can distort the profiles. The profiles obtained this way (with the exception of Fig. 3) are not shown. The remaining profiles had proper scale and offset values determined by a quick calibration observation and the uploaded into the correlator, improving the dynamic range. All future observations should be calibrated in this way.

¹<http://www.jb.man.ac.uk/~pulsar/Resources/epn/browser.html>

Strong pulsars observed with the Spigot have dips on either side of the pulse in their profiles (e.g., Fig. 3). These dips are artifacts due to 3-level sampling (Jenet & Anderson 1998), and may be aggravated by improper calibration. For observations of weak pulsars, such that a single pulse does not significantly change the system power, such artifacts do not occur, as can be seen in Figures 4 and 5.

We observed the binary millisecond pulsars (with the exception of PSR B1913+16) several times separated by spans from hours to days. We then folded the pulsars using available ephemerides and measured pulse arrival times. We found the arrival times to be generally consistent with a constant delay (Figs. 6–8), with rms scatters of a few microsecond (no observatory clock corrections were applied). There do appear to be some systematic trends for the second session of observations for PSR J0218+4252, but these are likely due to uncertainties in the ephemeris.

The tests that still need to be done are:

1. Test the modes with NLAGS \neq 1024
2. Test the modes with 50-MHz bandwidths
3. Figure out the setup for using 200-MHz bandwidths, and test
4. Test the modes with summed polarizations
5. Test the modes with multiple samplers
6. Test the modes with Stokes parameters

Of these, the first two should be simple and will likely not require any significant changes to the observing software. The third item does not depend on the observing software but depends on the spectrometer setup. Items 4-6 will require updates to the observing software.

REFERENCES

- Hobbs, G. B. & Manchester, R. N. 2003, ATNF Pulsar Catalogue, v1.2, (available on the World-Wide-Web at <http://www.atnf.csiro.au/research/pulsar/psrcat/>)
- Jenet, F. A. & Anderson, S. B. 1998, PASP, 110, 1467
- Kuiper, L., Hermsen, W., Verbunt, F., Ord, S., Stairs, I., & Lyne, A. 2002, ApJ, 577, 917

Table 1. Pulsars Observed with the Spigot: 2003-August-22, 23, 24

PSR	P (ms)	DM (pc cm ⁻³)	P_b (days)	S_{1400} (mJy)	Bits	ν_{RF} (MHz)	$\Delta\nu_{\text{RF}}$ (MHz)
J0218+4232	2.3	61.3	2.0	0.9	16	1375	150
B0329+54	714.5	26.8	...	203.0	16	9000	800
B0355+54	156.4	57.2	...	230	16	1375	150
					8	1375	150
					4	1375	150
					16	2000	320
J0613-0200	3.1	38.8	1.2	2.2	16	1375	150
					8	1375	150
					4	1375	150
J1012+5307	5.3	19.5	0.6	2.8	16	1375	150
B1929+10 ^a	226.5	3.2	...	41.0	16	1375	150
B1913+16	59.0	168.8	0.3	0.7	16	1375	150
B1937+21	1.6	71.0	...	16.0	16	1375	150

^aSimultaneous BCPM observations were taken.

Note. — Sampling times for 4, 8, and 16-bit modes were 20.48 μs , 40.96 μs , and 81.92 μs respectively. All observations used 1024 lags and a single 800-MHz bandwidth: the smaller RF bandwidths were set by IF filters.

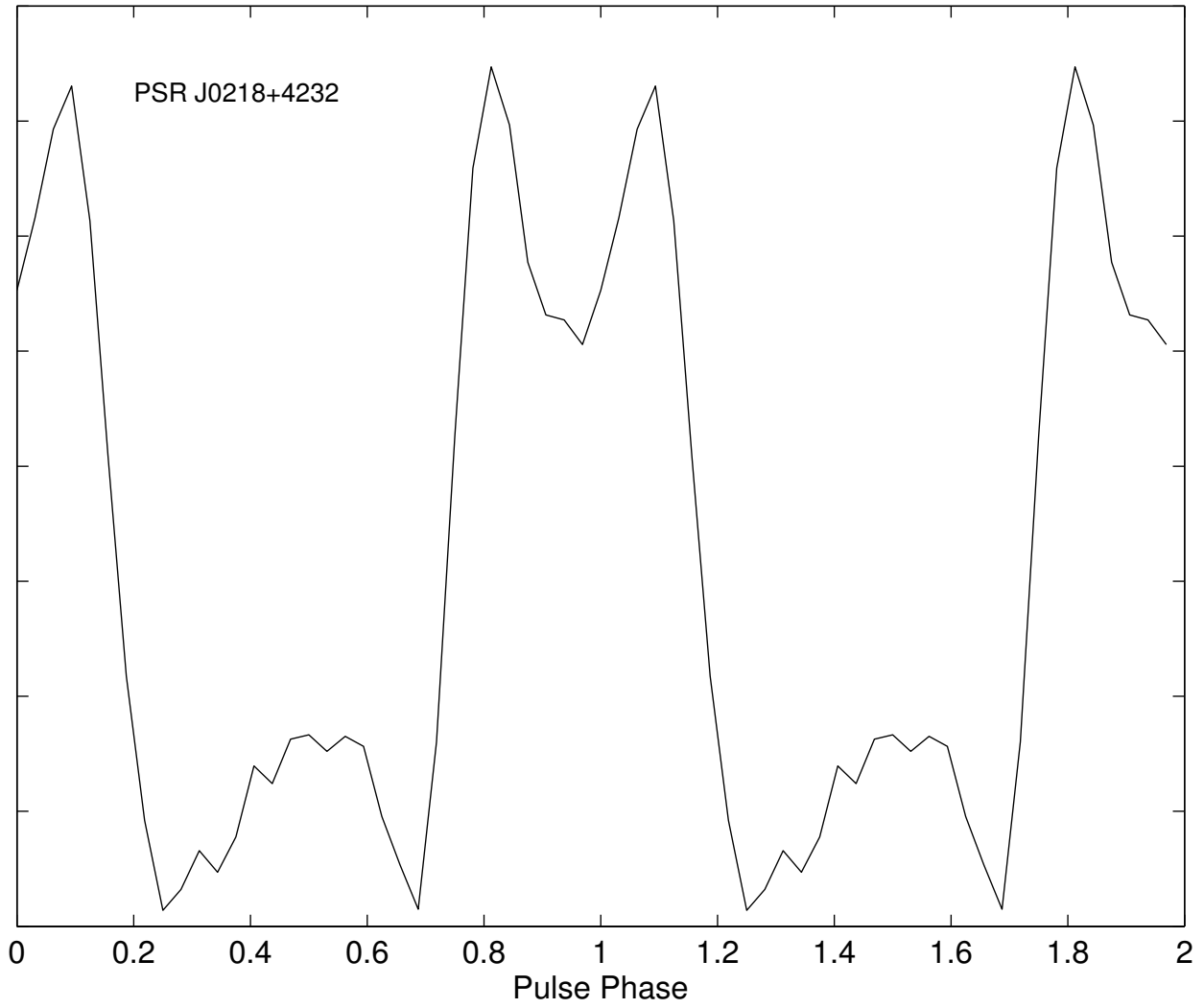


Fig. 1.— Pulse profile of PSR J0218+4232, repeated twice for clarity. The profile is similar to that observed previously (e.g., Kuiper et al. 2002).

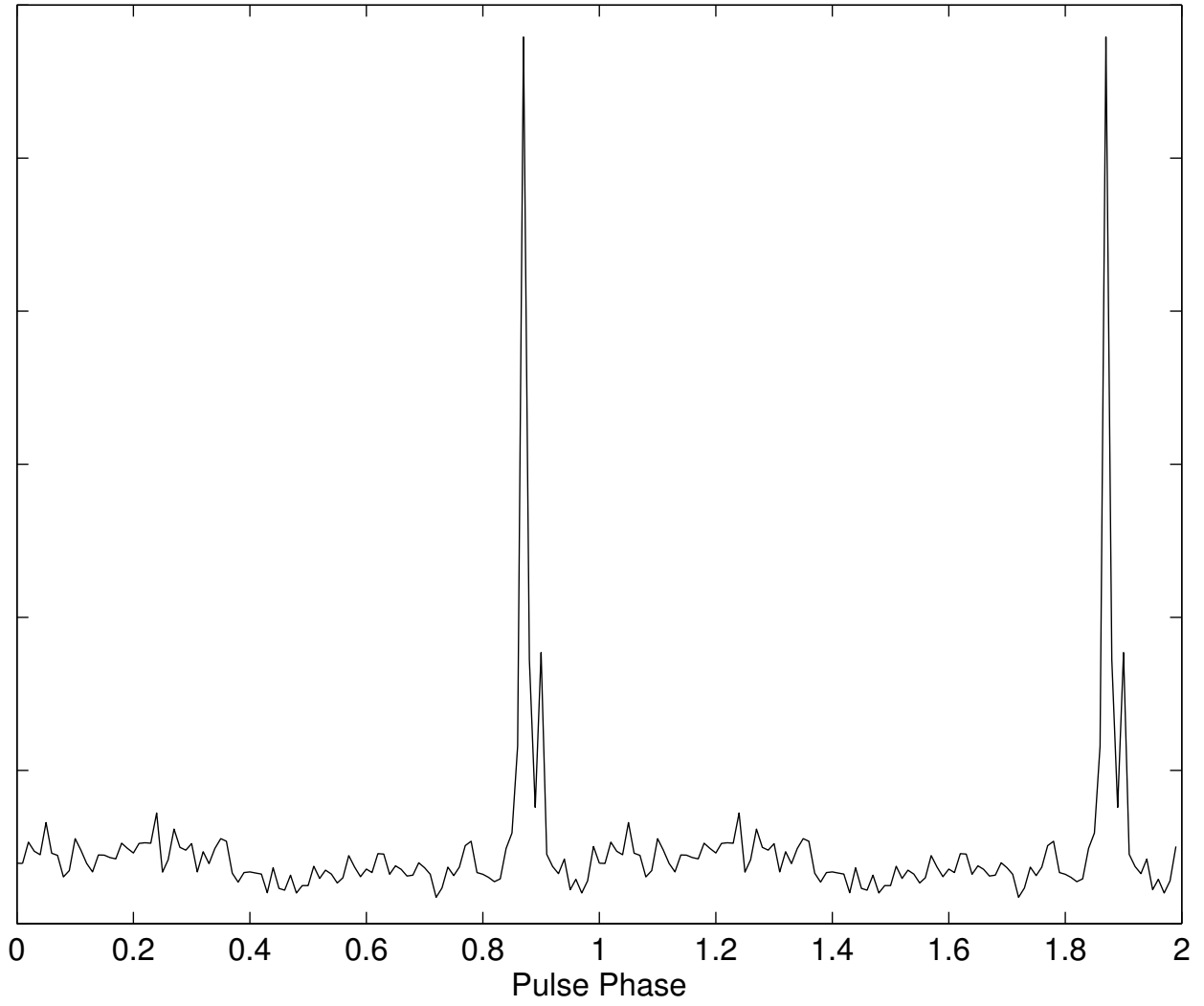


Fig. 2.— Pulse profile of PSR B0329+54, repeated twice for clarity.

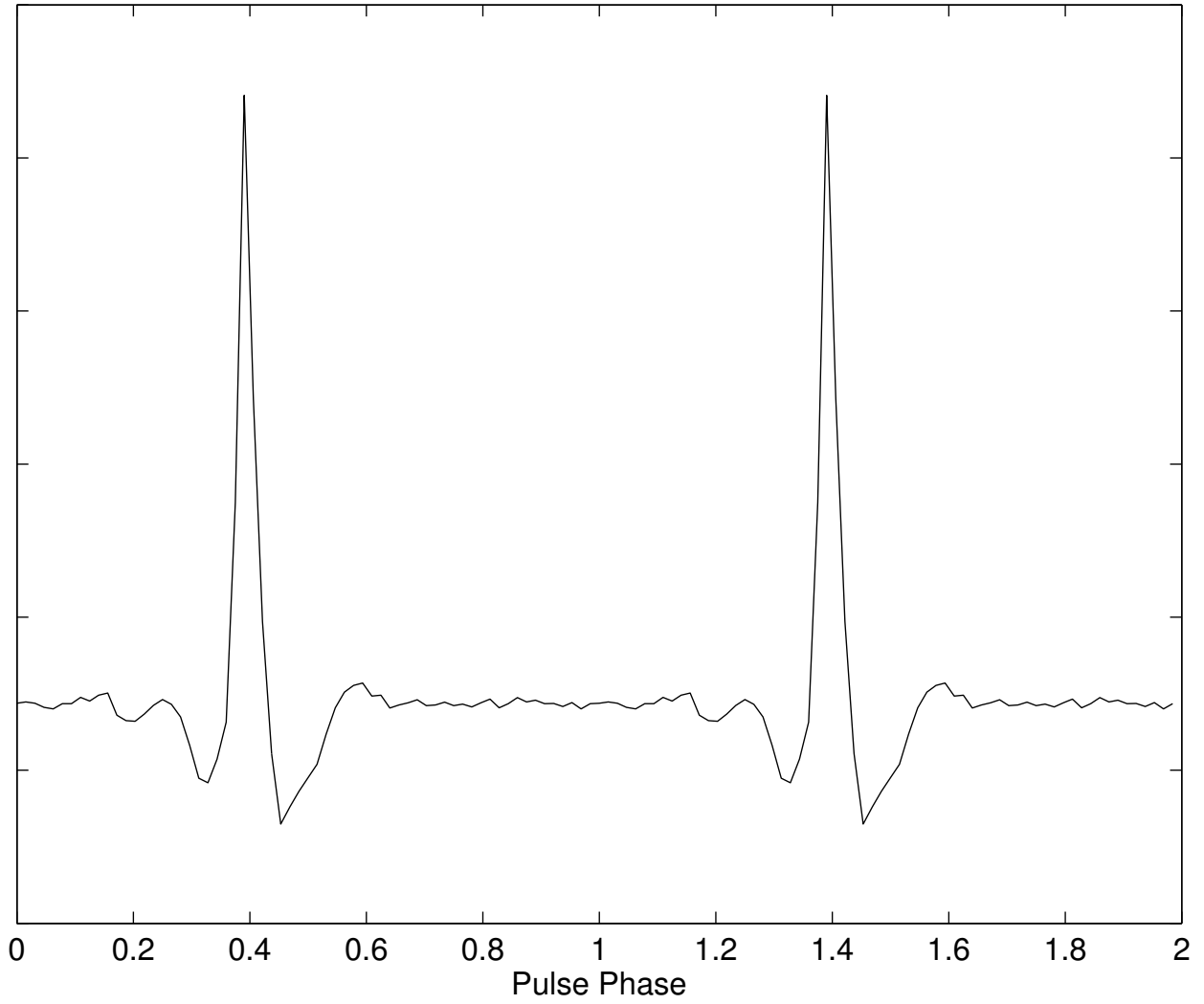


Fig. 3.— Pulse profile of PSR B0355+54, repeated twice for clarity. The dips in the baseline are due to 3-level sampling artifacts. This pulsar was not observed with optimal dynamic range.

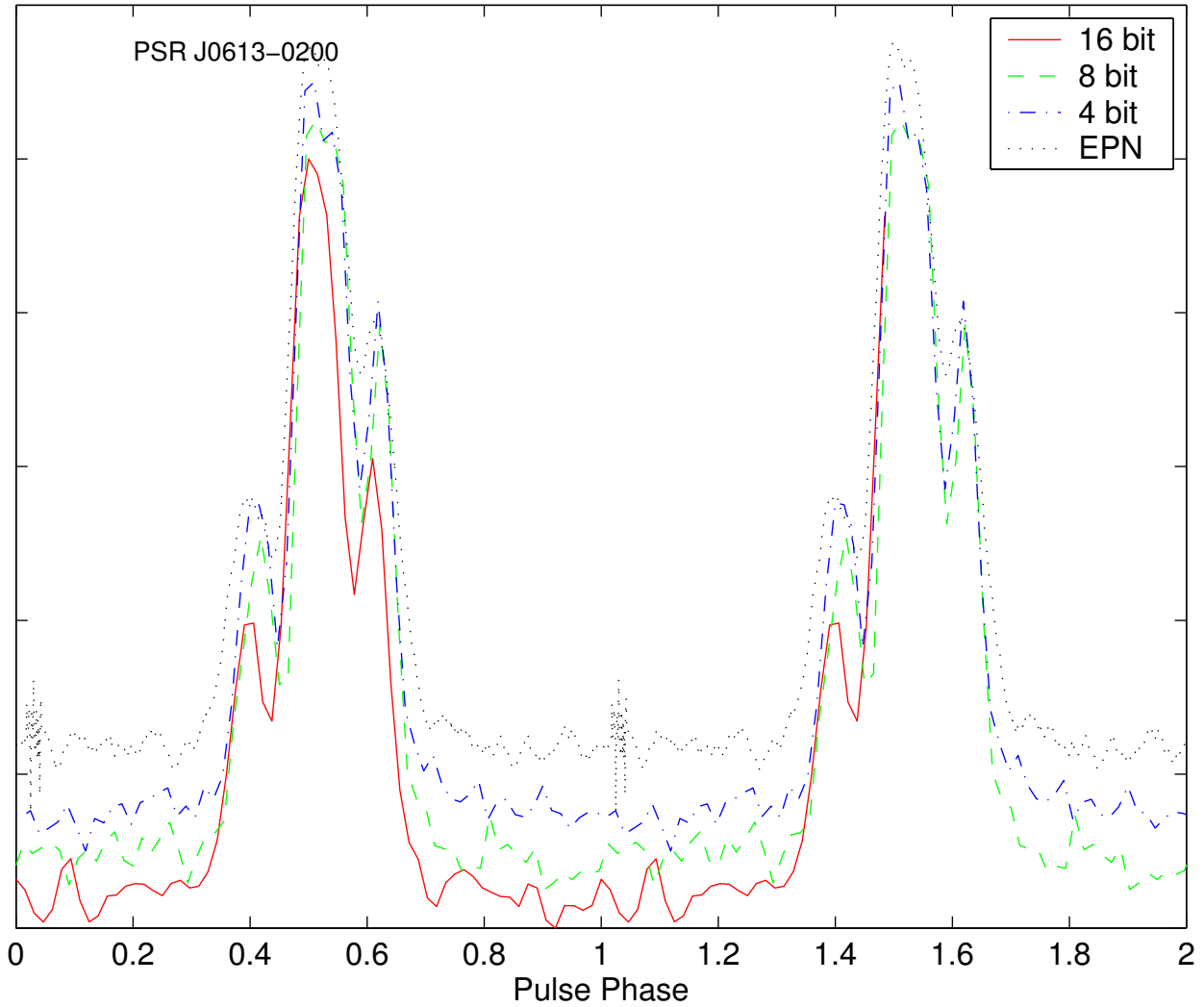


Fig. 4.— Pulse profile of PSR J0613–0200, repeated twice for clarity. The profiles shown are from 16-bit (solid red line), 8-bit (dashed green line), and 4-bit (dot-dashed blue line) modes, along with the 1.4-GHz EPN profile (black dotted line), where the 8 and 4-bit data are vertically offset for clarity.

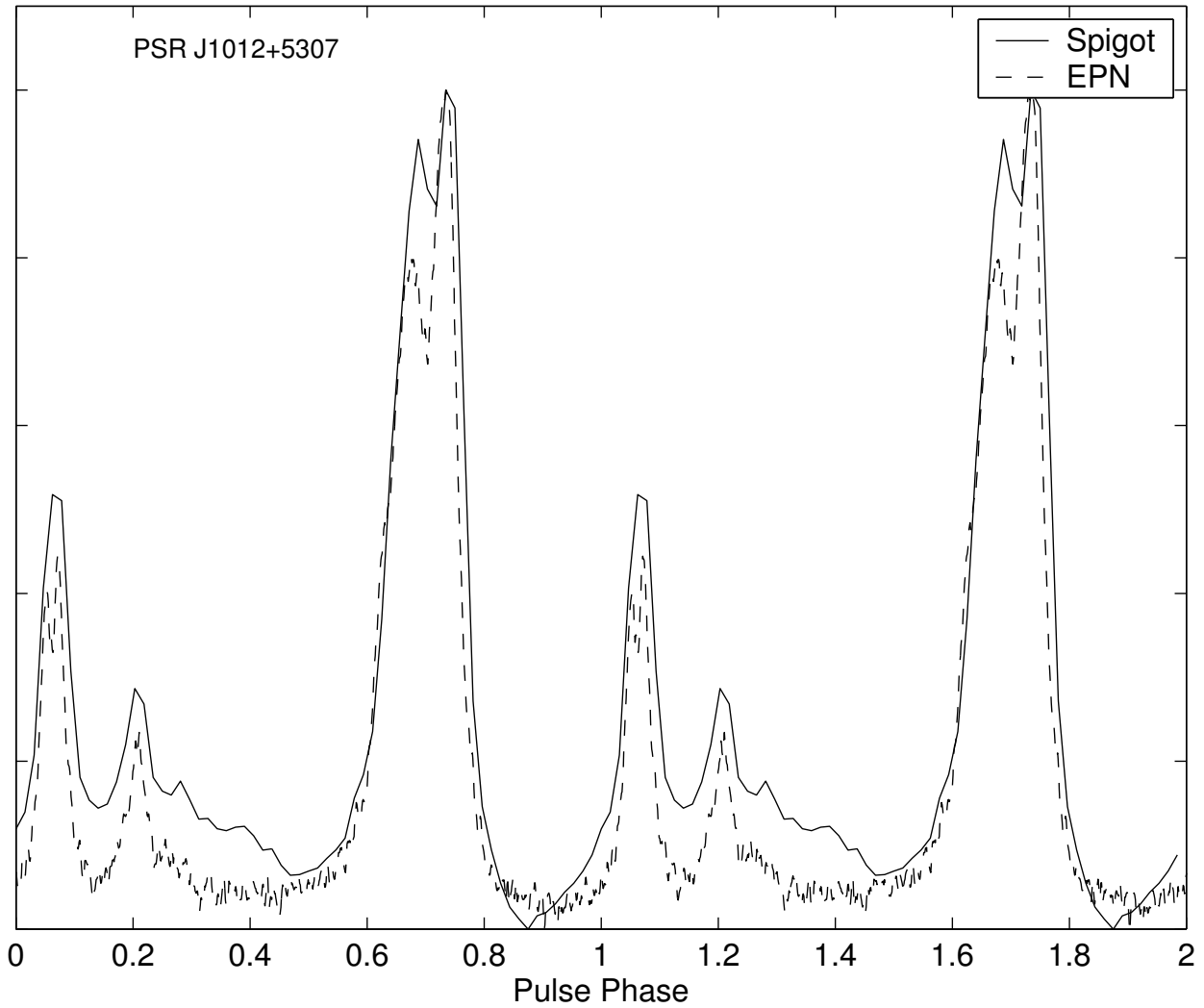


Fig. 5.— Pulse profile of PSR J1012+5307, repeated twice for clarity. The profiles shown are from the Spigot (solid line) and the EPN archive (dashed line).

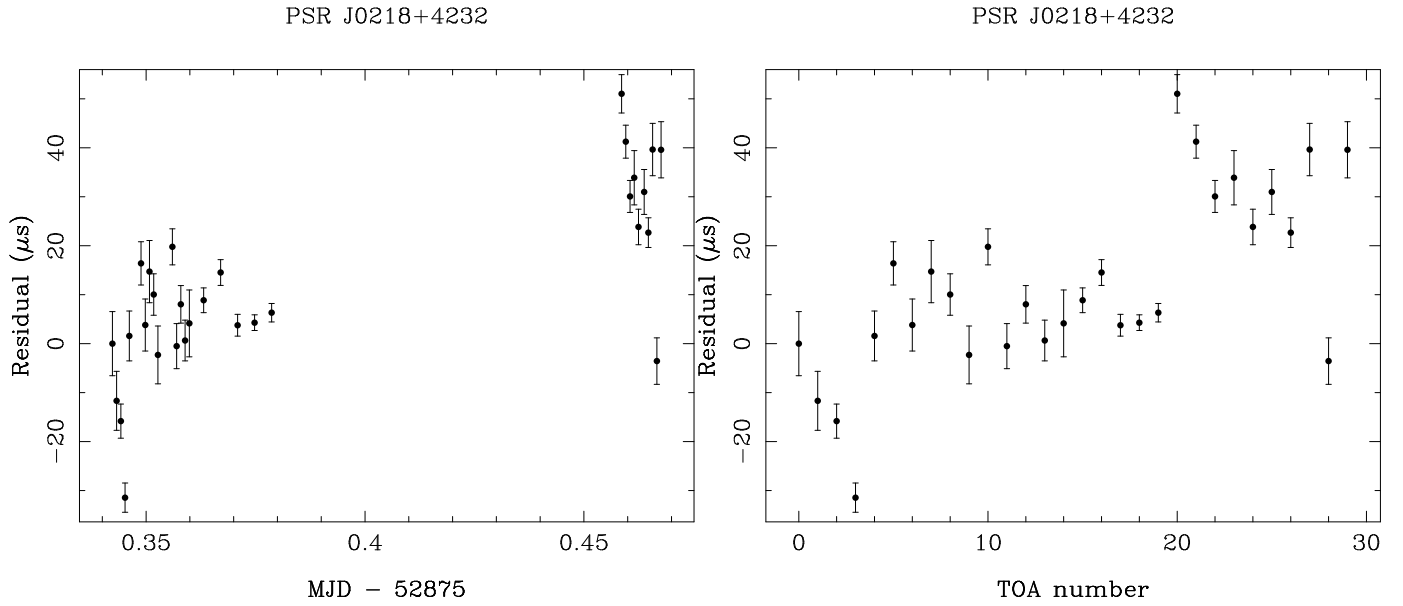


Fig. 6.— Pulse times-of-arrival (TOAs) from PSR J0218+4232, plotted as a function of MJD (left) and as a function of observation number (right). The pulsar was folded using the ephemeris from the ATNF pulsar database (Hobbs & Manchester 2003). The differences in the uncertainties between TOAs reflect different integration times.

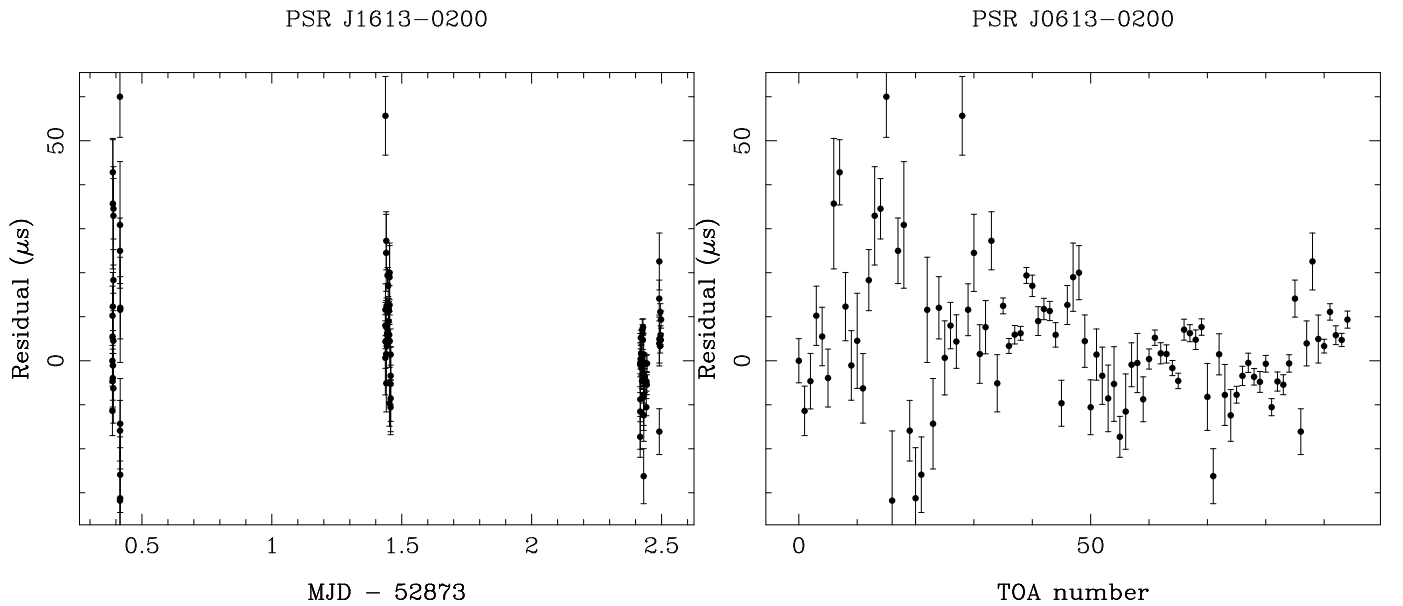


Fig. 7.— Pulse times-of-arrival (TOAs) from PSR J0613-0200, plotted as a function of MJD (left) and as a function of observation number (right). The pulsar was folded using the ephemeris from G. Hobbs (2003, personal communication). The differences in the uncertainties between TOAs reflect different integration times.

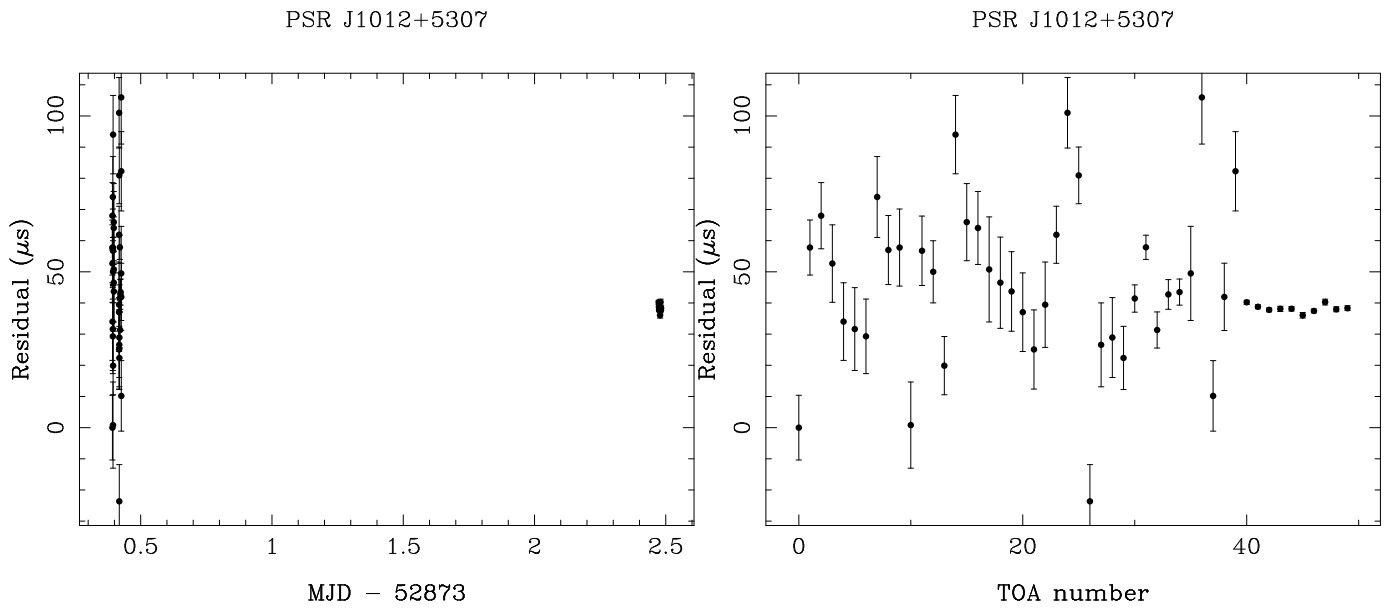


Fig. 8.— Pulse times-of-arrival (TOAs) from PSR J1012+5307, plotted as a function of MJD (left) and as a function of observation number (right). The pulsar was folded using the ephemeris from the ATNF pulsar database (Hobbs & Manchester 2003). The differences in the uncertainties between TOAs reflect different integration times.